iranpaper Downloaded from https://iranpaper.ir

Structures 33 (2021) 3382–3396

Contents lists available at ScienceDirect

Structures

journal homepage: www.elsevier.com/locate/structures

Effects of using different arrangements and types of viscous dampers on seismic performance of intermediate steel moment frames in comparison with different passive dampers

Reza Siami Kaleybar, Payam Tehrani *

Department of Civil and Environmental Engineering, Amirkabir University of Technology, Iran

ARTICLE INFO

Keywords:
Passive control systems
Viscous damper
Viscoelastic damper
Friction damper
Metallic damper
Damper arrangement

ABSTRACT

In this paper, the effect of using different passive control systems on the seismic performance of an eight-story intermediate steel moment frame was investigated. For this purpose, ten steel frames equipped with the linear and nonlinear fluid viscous dampers with three different arrangements, viscoelastic damper, Pall friction damper, and metallic damper (TADAS) were modeled and designed according to the ASCE 7-16 and AISC 360-16 provisions. To investigate the seismic behavior of each system, nonlinear time history analyses were performed using eleven ground motion records in OpenSees software. The seismic responses of the frames were studied and compared in terms of the maximum roof displacement, maximum story drift, maximum base shear, input energy, and dissipated energy through the dampers for different types and arrangements of dampers. The results revealed that the structures with dampers had an outstanding seismic performance compared to the original structure. Among the three arrangements considered for the viscous dampers, the toggle arrangement had a significantly better seismic performance compared to the Chevron and Diagonal damper arrangements. Also, nonlinear viscous dampers dissipated much more seismic input energy compared to linear viscous dampers that resulted in improved seismic performance of the frames. In addition, among the friction, metallic, and viscoelastic dampers, the friction damper had the most beneficial effects for the structures studied.

1. Introduction

Given the vulnerability of buildings in severe earthquakes, one of the challenges for engineers is always to use efficient equipments within the structure to dissipate seismic energy [1]. One solution could be passive energy damping devices, which damp the seismic energy without a need for an external energy source like electricity [2]. The primary role of these devices is to increase the overall stiffness and damping in the structure and thereby reduce displacement demand in the main members of the frame, such as beams and columns [3]. In conventional structural systems, due to the lack of energy dissipating systems, the earthquake input energy is dissipated through plastic deformation in structural elements such as beams and columns in moment-resisting frames, vertical or horizontal links in eccentrically braced frames (EBFs) and bracings in concentrically braced frames. The plastic deformation in the structural members can cause structural damage and may result in costly rehabilitation plans. Furthermore, if the structural damage exceeds certain limits the safety of the structure is endangered and structural collapse can occure. New design procedures have been proposed for such conventional systems to improve their seismic performance and their collapse mechanism [4–10].

Therefore, using energy-damping systems such as viscous, viscoelastic, friction, and metallic dampers is an excellent method to absorb the input seismic energy and save the structural elements from damage. These devices start to dissipate energy by either yielding of mild steel, sliding friction, the motion of a piston within a viscous fluid, or viscoelastic action in polymetric materials [1]. Because these devices require relative displacement or velocity to be activated, they can be categorized into two groups: displacement-dependent and velocity-dependent devices. Yielding of mild steel and friction-based devices are examples of the first group; also, viscous fluid damper and viscoelastic materials are in the second group [11].To date, some numerical and experimental works are performed to show how damping devices affect the seismic performance of the structures; for example, Constantinou and Symans [12] did an experimental study and compared the seismic response of a structure with and without fluid dampers. Lee and Taylor [13] explained

* Corresponding author.
E-mail addresses: reza.siami@aut.ac.ir (R. Siami Kaleybar), payam.tehrani@aut.ac.ir (P. Tehrani).

https://doi.org/10.1016/j.istruc.2021.06.079
Received 7 April 2021; Received in revised form 28 May 2021; Accepted 22 June 2021
Available online 29 June 2021
2352-0124/© 2021 Institution of Structural Engineers. Published by Elsevier Ltd. All rights reserved.

Downloaded from https://iranpaper.ir

fluid viscous damper and its technology, installation methods, and the analysis procedure. Uriz and Whittaker [14] studied the retrofitting of a pre-Northridge three-story steel frame with viscous dampers. Miyamoto et al. [15] investigated the collapse hazard of a ten-story steel frame equipped with a viscous damper during large earthquakes. Kim et al. [16] evaluated the progressive collapse potential of steel frames equipped with viscous dampers. Wang and Mahin [17] focused on retrofitting of a 35-story steel building with viscous dampers and proposed an optimized placement of these dampers. Sepehri et al.[18] studied the seismic demand of viscous dampers by focusing on the probability of damage in these devices. Gong et al. [19] investigated the seismic performance of an irregular and complex structure equipped with a new type of viscoelastic damper. Heydarinouri and Zahrai [20] proposed a step by step procedure for designing and determining optimal location of viscoelastic dampers. Liao et al.[21] compared results from the experiment and capacity spectrum method for a three-story steel frame equipped with a friction damper. Ribakov [22] investigated a hybrid damping system that contained viscous and friction dampers. Tafakori et al. [23] worked on retrofitting a 15-story steel structure equipped with a friction damper and optimized the damper's configuration. Brando et al. [24] studied hysteretic and viscous dampers in a three-story steel frame. Bagheri et al. [25] compared the seismic response of metallic and friction dampers in 3, 5, and 10-story structures. Tehrani and Maalek [26,27] compared the use of different types of passive dampers in seismic rehabilitation of an existing steel structure. Nastri et al. described three design criteria for moment-resisting frames (MRFs) equipped with friction beam-to-column joints and examined their seismic performance using non-linear static and dynamic analyses [28]; Mirzai et al. proposed a self-centering damper for inverted Y-braced EBF system that combines shape memory alloy bars and lead rubber damper (SMA-LRD) to reduce the link plastic rotation demand, residual link plastic rotation, maximum absolute floor acceleration and repair costs and it can also be used as a system for seismic retrofitting of the EBFs. [29]. Titirla et al. studied the mechanical response of an innovative energy dissipation device in which the energy dissipation mechanism of the superimposed blades functions via both steel yielding and frictional forces between the blades [30]. Piluso et al. proposed an innovative approach for the use of friction dampers in seismic resistant steel structures. They developed beam-to-column connections equipped with friction dampers showing low damage [31].

For the case of viscous dampers often different arrangements can be used for the installation of the dampers (e.g., diagonal, chevron and toggle arrangements) and in addition, the behavior of the dampers can be either linear or nonlinear. Some studies investigated the viscous dampers with toggle arrangements and proposed some criteria on the geometric properties of this arrangement [32–34]. Very limited research is available to investigate the influence of such properties of viscous dampers (i.e., different arrangements and types of behavior) on the seismic performance of steel frames. In the present study first the influence of arrangements and nonlinear behavior is investigated on the seismic response of steel frames equipped with viscous dampers and then the effects of using different passive control devices on the seismic performance of the frames are compared. In the next parts, the properties and applications of these devices are described briefly.

1.1. Viscous damper

Viscous dampers are usually constructed in two different ways, with an accumulator (Fig. 1a) or with a run-through piston rod (Fig. 1b). In the first method, silicon fluid within the cylinder, moves from a chamber to another chamber through orifices of the piston head. In the second method, which is more common than the first one, the fluid moves through the gap between the piston head and the cylinder. The motion of the fluid within the cylinder, which is induced by an external force like wind or ground motion, dissipates the input energy [35,36].

Also, the force in the fluid damper is specified as follows [11]:

$$F = C|\dot{u}|^{\alpha} \times sgn(\dot{u}) \tag{1}$$

where C is damping constant, $\dot{u}$ is the velocity of the piston, α is a coefficient in the range of 0.1 to 2.0, and sgn is the signum function. Dampers with $\alpha = 1$ are considered as a linear viscous damper. In addition, the viscous damper can be used in different arrangements such as diagonal, chevron, and toggle, as shown in Fig. 2 [33].

The additional damping ratio induced by a viscous damper can be determined with the following Equation [37]:

$$\zeta = \frac{T_1^{2-\alpha}\lambda\sum_j C_j\left|(f_h)_j(\varnothing_h)_{rj} - (f_v)_j(\varnothing_v)_{rj}\right|^{1+\alpha}}{(2\pi)^{3-\alpha}A^{1-\alpha}\sum_i m_i(\varnothing_h)_i^2} \tag{2}$$

where T_1 is the fundamental natural period of the structure, C_j is the damping coefficient, $(\varnothing_h)_{rj}$ is the first mode relative displacement in the horizontal direction, $(\varnothing_h)$ is the modal displacement normalized to a unit value at the roof; A is the roof displacement, m_i is the weight of each story, f_h is the magnification factor, and λ is a coefficient which is determined as follows:

In which Γ is the gamma function. It should be noted that in this research, $(f_v)_j(\varnothing_v)_{rj}$ term in Equation (2) was not considered due to ignoring the vertical displacement of the structure.

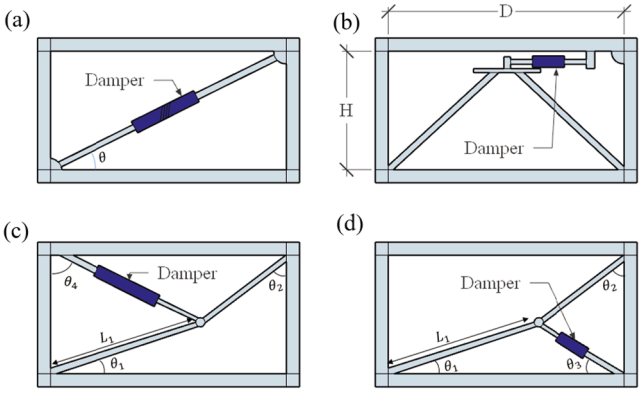

Fig. 2. Different arrangements of viscous damper: (a) diagonal, (b) chevron, (c) upper toggle system, and (d) lower toggle system [33].

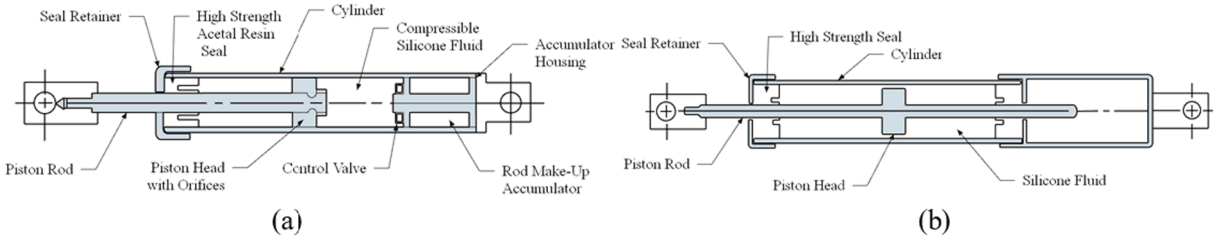

Fig. 1. Viscous damper configurations: (a) with an accumulator and (b) with a run-through piston rod [35,36].

iranpaper Downloaded from https://iranpaper.ir

1.2. Viscoelastic damper

Viscoelastic dampers, unlike the viscous dampers, conduce a considerable increase in stiffness of the structure in addition to increasing damping. Also, these devices spread the input energy in a wider frequency range. The typical construction of these devices is shown in Fig. 3, which is made from viscoelastic layers, and a steel plate accommodates between them. It is worth mentioning that the dissipation of energy in these devices is a result of the shear deformation of viscoelastic materials [35].

In general, the viscoelastic damper properties depend on the storage modulus G', loss modulus G'', and loss factor η_v, etc. After adding the viscoelastic damper to the model, if the mode shapes had no noticeable changes, the following Equation can be used for calculation of damping ratio, ξ_i, for the i^{th} vibration mode [38]:

$$\xi_i = \frac{\eta_{v-b}}{2}\left(1 - \frac{\omega_i^2}{\omega_{si}^2}\right) \tag{4}$$

In which ω_{si} and ω_i are the i^{th} natural frequencies of the structure with and without a viscoelastic damper, respectively; and η_{v-b} is the total effective loss factor of the viscoelastic dampers.

1.3. Friction damper

Friction dampers generally are constructed by clamping steel plates together. The friction mechanism between the plates dissipates input energy. These dampers are designed for an optimum slip load so that the main members do not yield before dampers slip. If the slip load is chosen very low or very high, as shown in Fig. 4, the response would be irrational, and maybe after an earthquake, the structure will not return to the elastic state. In this research, a Pall friction damper is used, which is shown in Fig. 5 [39]. Some of the advantages of these types of dampers are noticed as follows [40]:

- Low cost and no requirement for any maintenance
- No need to replace or repair after an earthquake
- Providing additional damping and stiffness to structure and making it more sustainable
- Independent performance on various temperature and velocity
- Not suffering from fatigue
- Easy accommodation within the structure

1.4. Metallic damper

Metallic dampers dissipate the input energy by yielding of metals. The mechanism of these devices is based on the relative drift between the upper and lower ends of plates. TADAS is one of these dampers that is shown in Fig. 6. Some of the advantages of these dampers are the simple construction, easy accommodation in the frame, having stable

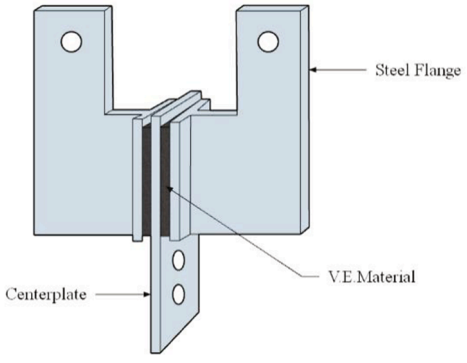

Fig. 3. Viscoelastic damper configuration [35].

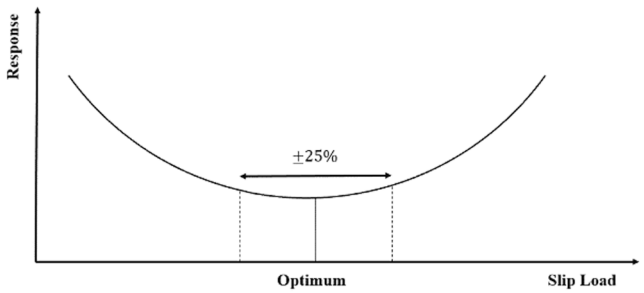

Fig. 4. Friction damper slip load [39].

behavior during an earthquake, easy to replace, not dependent on environmental changes, and adding additional damping and stiffness to the structure [41].

One of the essential issues that should be considered in the design of these devices is low-cycle fatigue. The number of cycles (N_f) that can be tolerated until reaching the plastic strain (ε_{max}) in these devices can be determined by the following Equation [42]:

$$\varepsilon_{max} = AN_f^{-b} \tag{5}$$

where A = 0.08, b = 0.3, and N_f = 100 are considered for steel devices. Moreover, the Shear strength (V_d) of each plate can be determined by Equation (6) [42]:

$$V_d = \frac{F_y bt^2}{4h} \tag{6}$$

In which F_y is the yield stress of metal, b is the width, t is the thickness, and h is the height of the triangular plate. Also, the stiffness of each plate can be calculated by the following Equation [42]:

$$K_{di} = \frac{Ebt^3}{6h^3} \tag{7}$$

In which E is the metal modulus of elasticity.

1.5. Hysteresis loops of dampers

In Figs. 7 and 8, force–displacement loops for displacement-dependent and velocity-dependent devices are shown, respectively [11]:

2. Model selection and assumptions

In this paper, a total of ten 2D eight-story steel intermediate moment frames equipped with different types of dampers were studied (i.e., one frame with no damper, six with linear and nonlinear viscous dampers in three different arrangements, one with viscoelastic, one with friction, and one with a metallic damper). Each frame has three bays with a length of 6 m (i.e., a total width of 18 m). The height of each floor was considered 3.2 m. The different arrangements of these models are shown in Fig. 9 and Fig. 10.

It was assumed that the structures are located on a site class C with seismic design category IV, S_{DS} = 1.579, and S_{D1} = 0.657. The structures were modeled and designed according to ASCE 7-16 code, AISC 360-16 provisions, and the seismic provisions of AISC 341-16 [43–45]. In accordance with ASCE7-16, steel structures with intermediate moment-resisting systems have response modification factor, R, over-strength factor, Ω_0, and deflection amplification factor, C_d, equal to 4.5, 3.0, and 4.0, respectively [43]. Eleven maximum direction spectra (RotD100 Sa(g)) were selected and scaled based on the ASCE7-16 provisions, such that the average of the maximum-direction spectra from all the ground motions generally matches or exceeds the target response spectrum over the period range of 0.2 T to 2 T, where T is the fundumental period of the structure. The average of the maximum-direction spectra from all the ground motions does not fall below 90% of the

Downloaded from https://iranpaper.ir

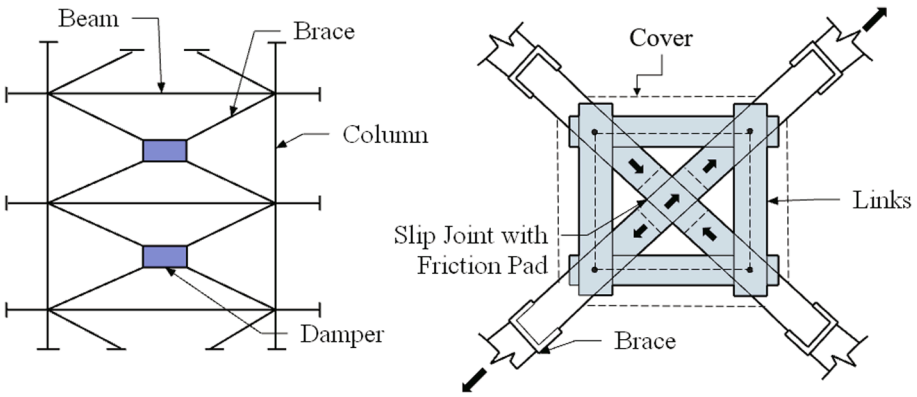

Fig. 5. Pall Friction damper configuration [39].

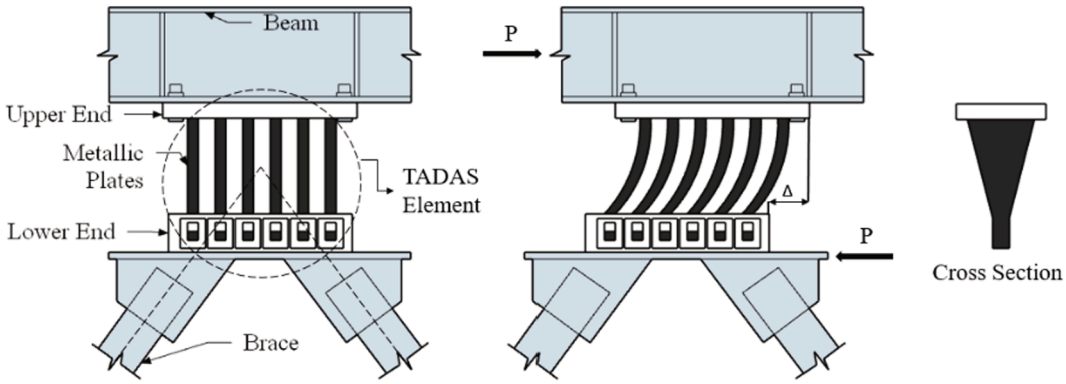

Fig. 6. TADAS configuration [41].

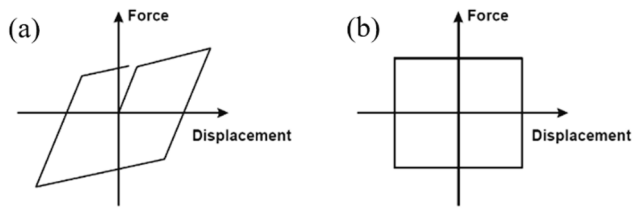

Fig. 7. Force-displacement loops for displacement-dependent devices: (a) metallic and (b) friction [11].

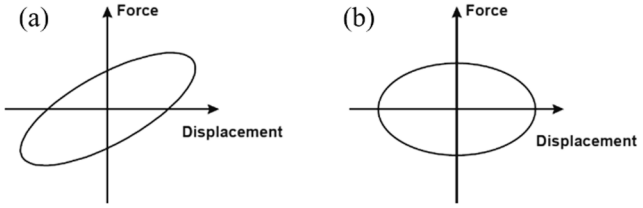

Fig. 8. Force-displacement loops for velocity-dependent devices: (a) visco-elastic and (b) viscous [11].

target response for any period within the same period range [43]. These eleven ground motions are imposed on all frames with the same scale factors. The properties of selected ground motions are depicted in Table 1, and the response spectra of the scaled ground motions are shown in Fig. 11.

The Metal deck system was used for floors, so the gravity dead loads were considered 4.9 and 4.0 kN/m^2, and the live loads were considered 2.0 and 1.5 kN/m^2, respectively, for the stories and the roof. It was assumed that the weight of the external walls is 11 kN/m. For performing 2D analysis, the procedure proposed by FEMA P695 was used to separate the 2D model from its 3D model. In accordance with this procedure, gravity loads are distributed to the outer beams with considering their tributary area. Also, to consider P-Delta effects, some leaning columns, which carry half of the gravity loads of each story, were modeled adjacent to the 2D frame [46]. Fig. 12 illustrates this method in a clear way. The columns and beams sections are BOX and IPE, respectively. The designed sections assigned to each story are shown in Table 2 that were determined from an equivalent lateral force procedure in SAP2000 software [47]. All of the intermediate moment-resisting frames in this study were designed using a behavior factor of 4.5 based on the ASCE 7-16 provisions. Also based on the ASCE7-16 provisions, the main elements of the equipped structures should tolerate 75% of the design base shear when the dampers do not work [43]. After designing the frames, a target damping ratio for the structures were considered (e.g., 15%) and the dampers were designed to achieve this damping ratio (e.g., as shown in Section 3). Since a similar R factor is used for the design of all frames, a more rational comparison can be made between the seismic performance of the frames equipped with various types of dampers for the sake of this research. It should be mentioned that SAP2000 version 22.2.0 and OpenSees version 3.2.2 were utilized for numerical modeling of these structures [47,48].

In SAP2000, the elements were modeled using super elements and concentrated hinges that are located at 5% of the length of the elements relative to both ends. The moment–curvature relation backbone curves (Fig. 13) for these hinges are defined by Table 9.7.1 of ASCE41-17 [49].

In OpenSees, a distributed plasticity method was utilized for modeling the frame members. For this purpose, each element should have enough fibers to be capable of catching nonlinear behavior. The number of integration points was considered equal to 5. It is noted that the optimal number of fibers and integration points were determined

Downloaded from https://iranpaper.ir

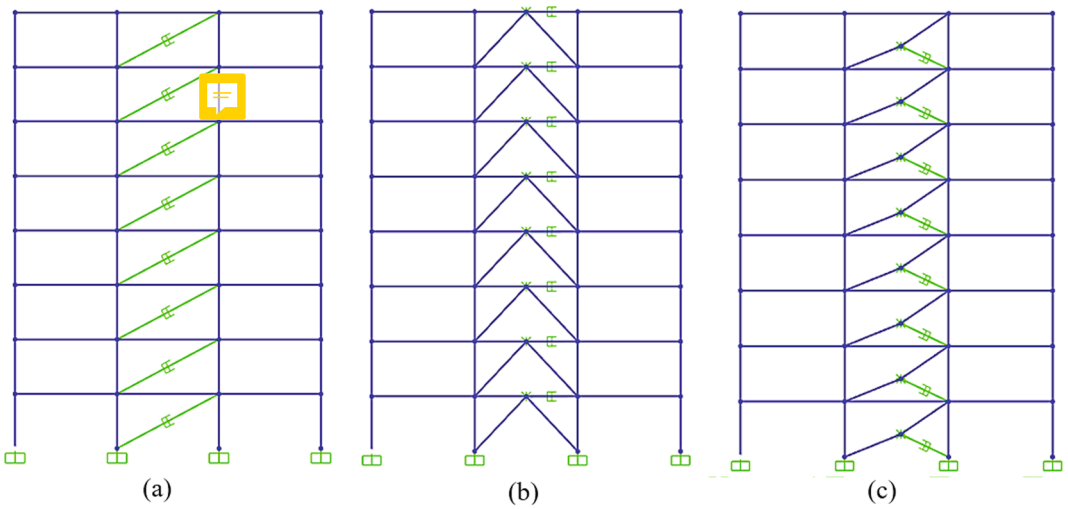

Fig. 9. Different arrangement of linear and nonlinear viscous damper: (a) Diagonal, (b) Chevron, and (c) Toggle.

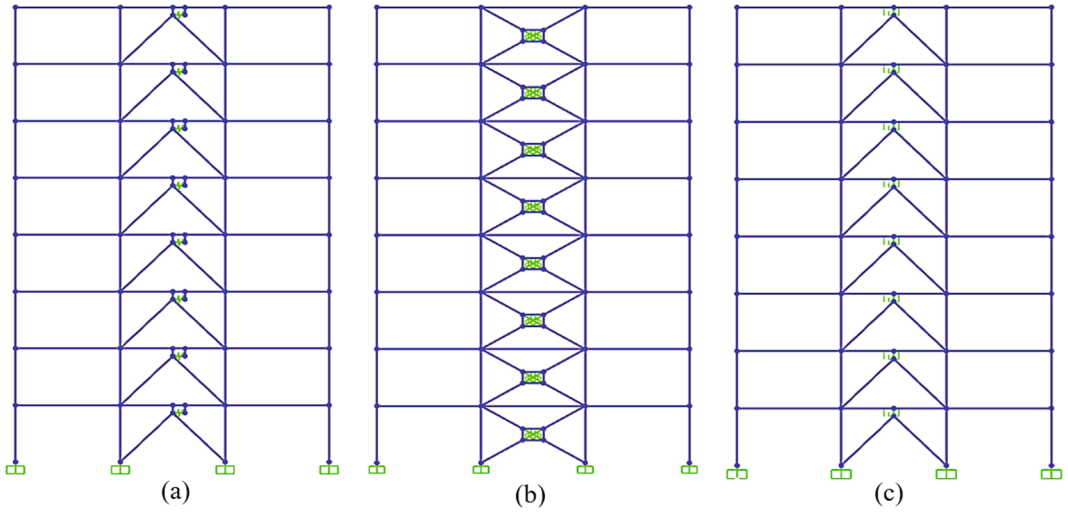

Fig. 10. Arrangement of (a) Viscoelastic, (b) Friction, and (c) Metallic dampers.

Table 1
Selected ground motions.

ID	Earthquake Name	Year	Station Name	Magnitude	Rjb (km)	Rrup (km)	PGA (g)	Scale Factor
1	Northridge-01	1994	Arcadia - Arcadia Av	6.69	39.41	39.73	0.10863	5
2	Hector Mine	1999	Amboy	7.13	41.81	43.05	0.21116	3
3	Imperial Valley-06	1979	Calexico Fire Station	6.53	10.45	10.45	0.28740	2.5
4	Kobe_ Japan	1995	Sakai	6.9	28.08	28.08	0.15998	3.4
5	Landers	1992	Mission Creek Fault	7.28	26.96	26.96	0.14706	5
6	Loma Prieta	1989	Coyote Lake Dam	6.93	20.44	20.8	0.30401	2
7	Chi-Chi_ Taiwan-03	1999	TCU075	6.2	18.47	19.65	0.25036	3
8	Cape Mendocino	1992	Fortuna Fire Station	7.01	16.54	20.41	0.41413	1.5
9	San Fernando	1971	LA - Hollywood Stor FF	6.61	22.77	22.77	0.25857	3
10	Superstition Hills-02	1987	Brawley Airport	6.54	17.03	17.03	0.14916	4.5
11	Friuli_ Italy-01	1976	Tolmezzo	6.5	14.97	15.82	0.39665	1.75

using a number of sensitivity studies to make sure that the predictions are accurate and precise. The details of these fiber sections for beams and columns are shown in Fig. 14. Steel02 material was used for modeling the behavior of steel, and the forceBeamColumn command was considered for nonlinear modeling of the main elements [48].

The structure material is ST52 with the yield strength of 360 MPa, Ultimate strength of 520 MPa, and a modulus of young equal to 200 GPa.

3. Dampers design and modeling

In this part, the detail of the design procedure and elements used for each damper are discussed. The elements, materials, and the restraint condition for joints and dampers are shown in Fig. 15 for each model.

iranpaper Downloaded from https://iranpaper.ir

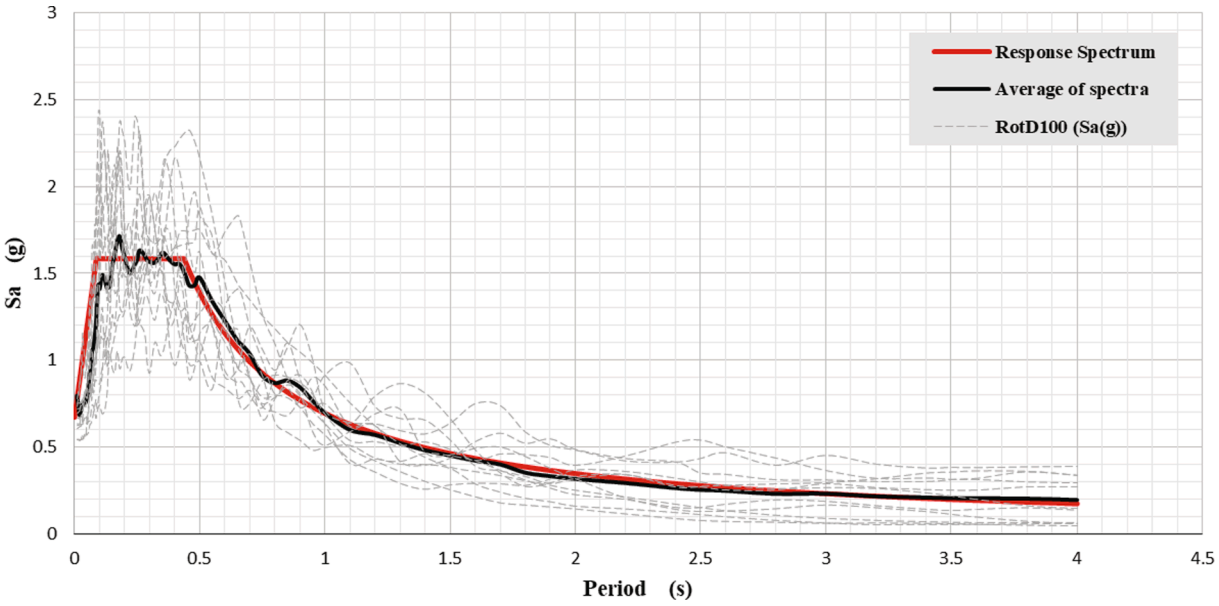

Fig. 11. Target response spectrum and scaled ground motion spectra.

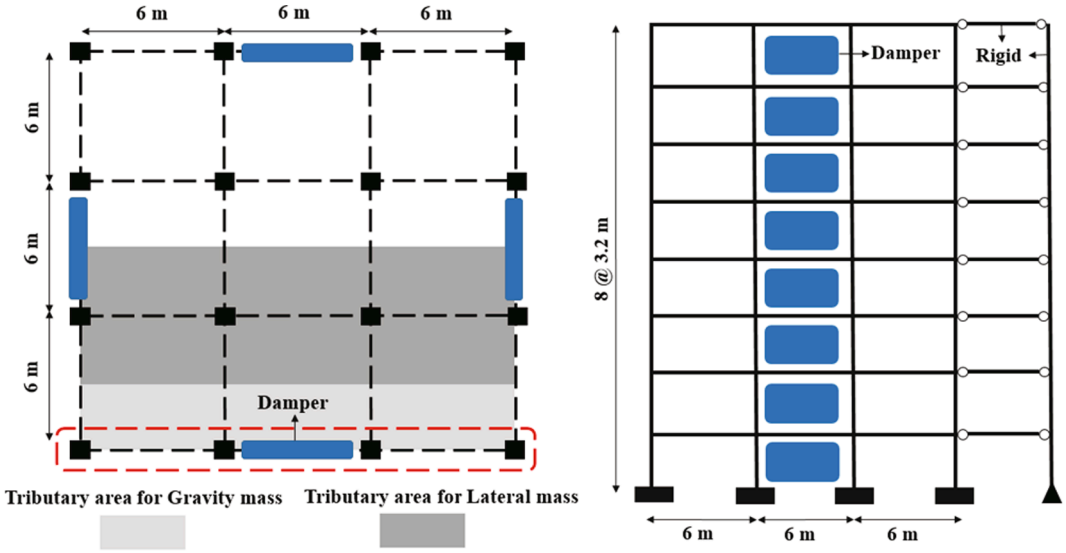

Fig. 12. Schematic plan and elevation of frames.

3.1. Viscous damper

In Fig. 15a,b, and c, the different arrangements of the viscous dampers are shown. For nonlinear and linear models of viscous damper, the α coefficient was considered as 0.5 and 1.0, respectively. Also, the λ coefficient was calculated using Equation (3), which is equal to 3.496 and 3.14 for nonlinear and linear models, respectively. The magnification factor for each arrangement is represented in Table 3 [42]. In the toggle arrangement, which is shown in Fig. 2d and Fig. 15c, the parameters were defined as below:

$\theta_1 = 22, \theta_2 = 55.56, \theta_3 = 26.42, L_1 = 3.5\text{m}, L_2 = 3.34\text{m}$

Research has shown that the magnification factor, f_h, in the range of 2 to 3 will typically result in an optimal performance and the toggle-brace-dampers with this range of f_h have been used in different research (e.g., Constantinou et al., 2001 and Zhang et al., 2012)[32,33]. Similarly, in this study the angles are selected so that the magnification coefficient is equal to 2.86, which is a reasonable value for the sake of this research. Also the criteria used for choosing the angles θ_1 to θ_3 of the toggle arrangement, as shown in Fig. 2 (d), are in accordance with a study by Hwang et al. (2005)[34].

It should be mentioned that in Fig. 15b, the distance between point A and the upper beam is equal to 1 cm; so the viscous damper can be assumed horizontally in the chevron arrangement.

The damping coefficient, C, is calculated from Equation (2), assuming an additional damping ratio, ζ, equal to 15%. In Table 4, the values of C are presented.

In SAP2000 software, "two joint link" element and "Damper-Exponential" link were used for modeling viscous damper in all arrangements.

In OpenSees, for diagonal arrangement, "twoNodeLink" element and "ViscousDamper" material were used. Also, for chevron and toggle arrangements "twoNodeLink" element and "Viscous" material were utilized. Braces are modeled using "elasticBeamColumn" command that are moment-free in both ends. It should be mentioned that the dampers can move only in U1 direction.

Downloaded from https://iranpaper.ir

Table 2
Designed sections.

ID	Frame	Story	Columns	Story	Beams	Story	Braces
		1–2	BOX 260	1–3	IPE 400	1–8	–
1	Without Damper	3–4	BOX 240	4–5	IPE 360		
		5–6	BOX 220	6–8	IPE 330		
		7–8	BOX 180				
2	Viscous-Diagonal-Linear						
3	Viscous-Diagonal-nonlinear						
4	Viscous-Chevron-Linear	1–2	BOX 260	1–3	IPE 400	1–8	2 UPN180
		3–4	BOX 240	4–5	IPE 360		
5	Viscous-Chevron-nonlinear	5–6	BOX 220	6–8	IPE 330		
		7–8	BOX 180				
6	Viscous-Toggle-Linear						
7	Viscous-Toggle-nonlinear						
8	Viscoelastic						
9	Friction	1–2	BOX 260	1–3	IPE 400	1–8	2 UPN200
10	Metallic	3–4	BOX 240	4–5	IPE 360		
		5–6	BOX 220	6–8	IPE 330		
		7–8	BOX 180				

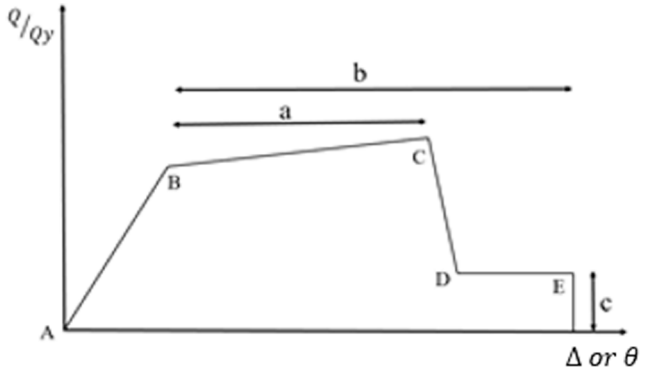

Fig. 13. Hinge Properties for frame elements [49].

3.2. Viscoelastic damper

In this article, according to Chang et al.(1998) study, 3MISD110 viscoelastic material was used, which has a storage modulus ($G^{'}$) and loss factor ($G^{''}$) determined as follows[38]:

$$G^{'} = e^{10.17443}.T^{-3.10205}.F^{0.475466}, \eta_v = \frac{G^{''}(\omega)}{G^{'}(\omega)} = 1.2 \quad (8)$$

Where T is the temperature in Celsius degree, and F is the frequency (Hz).

For designing this type of damper, the modal strain energy method was utilized [38]. According to this method and the study of Chang et al. (1998), two-layer of viscoelastic material with dimensions of 70, 50, and 5 cm for length, width, and thickness were determined, respectively. Also, the damping coefficient and the stiffness of the viscoelastic damper were calculated as 2641 $\frac{kN.Sec}{m}$ and 6189 $\frac{kN}{m}$, respectively.

In SAP2000 software, "two joint link" element and "Linear" link were used for modeling viscoelastic damper.

In OpenSees, two parallel "twoNodeLink" elements with "Viscous" and "Elastic" materials were used for modeling of the viscoelastic damper. Braces are modeled using "elasticBeamColumn" command, which are moment-free in both ends. The rigid elements were modeled using "rigidLink" command. It should be mentioned that the damper can move only in U1 direction. Details of modeling for this damper is shown in Fig. 15d.

3.3. Friction damper

In this study, for designing of friction dampers, the method proposed by Filiatrault and Cherry's (1990) was utilized [50]. Based on this method, the design slip load spectrum, as shown in Fig. 16, was determined. In this Figure, T_g is predominant ground period, T_u is the natural period of the unbraced structure that is equal to 2.285 sec, V_0 is the total optimum slip shear of all friction dampers in the structure, m is the total mass of the structure, and a_g is the peak ground acceleration. By using this spectrum, V_0 was determined as 1737 KN. After the distribution of V_0 to stories and dampers, each friction damper has an optimum slip load equal to 254 KN. It should be mentioned that all requirements for using this method were checked to be within limits. Also, it was checked that under wind load, friction dampers do not slip. In addition to these controls, it was checked that the braces do not yield before slipping of friction dampers [50].

In SAP2000 software, "two joint link" element and "Plastic Wen" link were used for modeling friction damper.

In OpenSees, "twoNodeLink" element with "BoucWen" material was used for modeling the friction damper. Braces are modeled using "elasticBeamColumn" command, which are moment-free in one end that is connected to the beam and column. It should be mentioned that the dampers can move only in U1 direction. Details of modeling for this damper is shown in Fig. 15e.

3.4. Metallic damper

The design of these dampers in this research was conducted based on

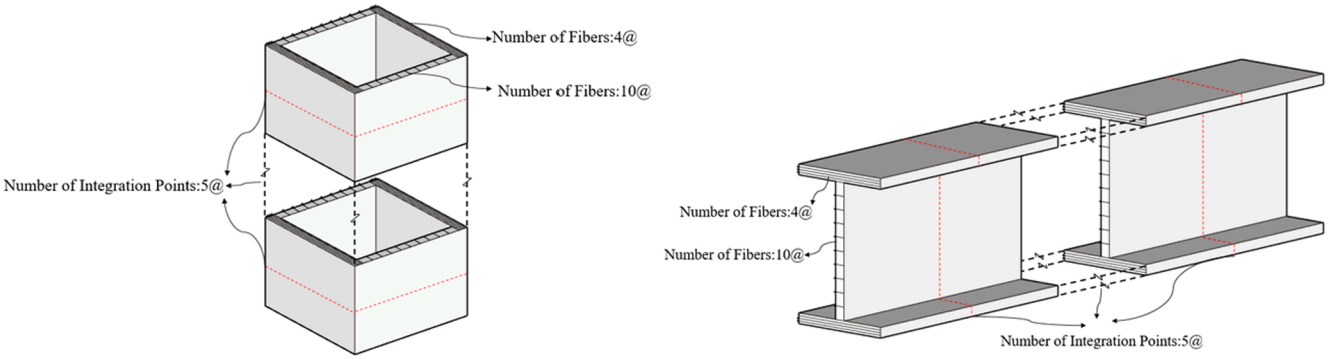

Fig. 14. Beam and column sections.

Downloaded from https://iranpaper.ir

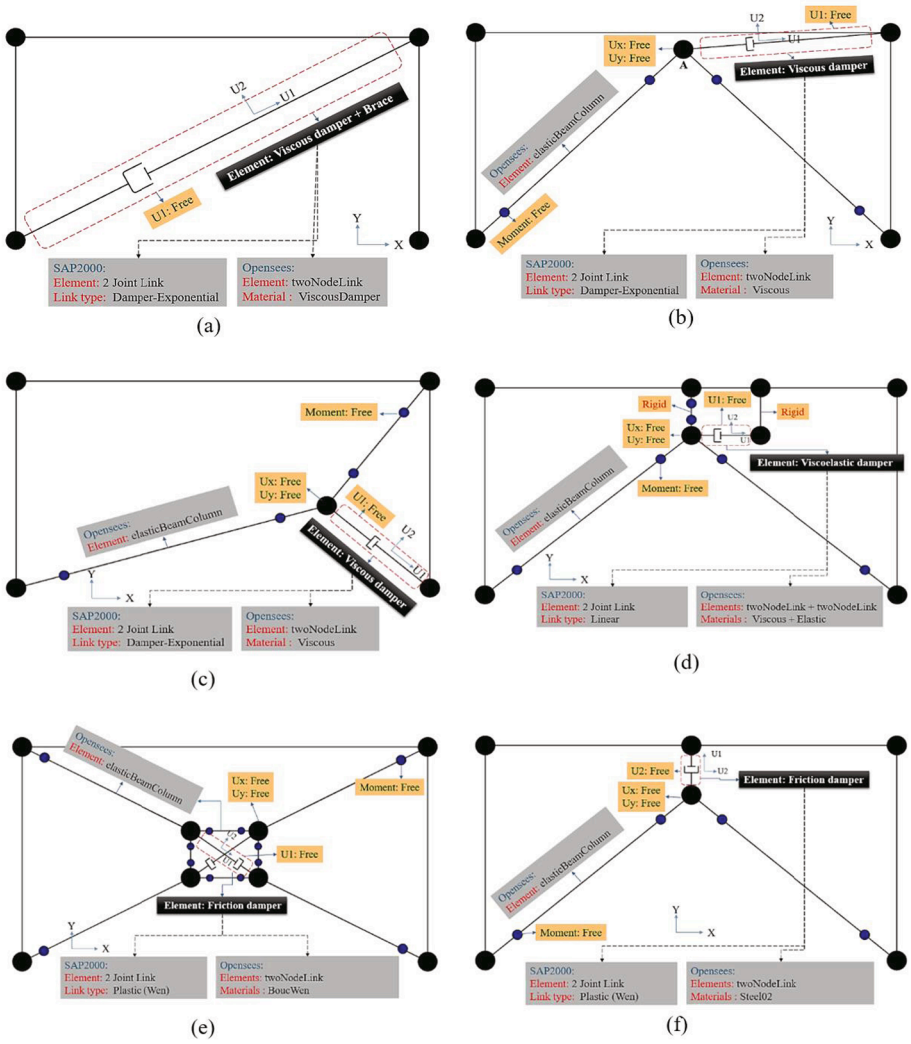

Fig. 15. Details of modeling for different types of dampers:a) Diagonal viscous damper b) Chevron viscous damper c) Toggle viscous damper d) Viscoelastic damper e) Friction damper f) Metallic damper.

Table 3
Value of f_h for each arrangement.

Arrangement	The formula for calculation of f_h	Value of f_h
Diagonal	$cos\theta$	0.8823
Chevron	1	1
Toggle	$\frac{sin(\theta_2)sin(\theta_1+\theta_3)}{cos(\theta_1+\theta_2)}$	2.8638

Table 4
Value of C for each arrangement.

Arrangement	Type	Value of C $\left(\frac{kN.Sec}{m}\right)$
Diagonal	Linear	3157
	Nonlinear	845
Chevron	Linear	2458
	Nonlinear	700
Toggle	Linear	298
	Nonlinear	144

a study by Tsai et al. (1993) [51]. By using Equations (5) to (7), the procedure proposed by Tsai (1993), and the ASCE7-16 code, the yield strength and stiffness for each damper were calculated and are summarized in Table 5:

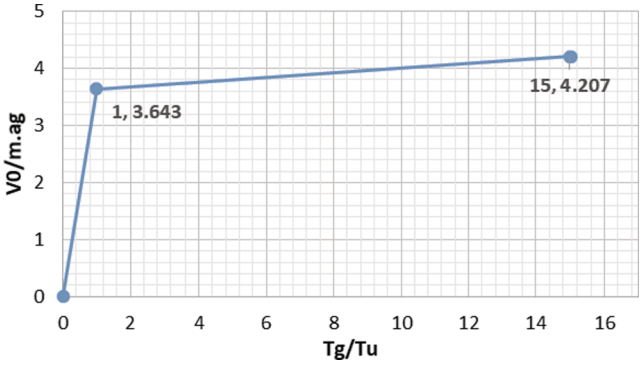

Fig. 16. Design slip-load spectrum.

In SAP2000 software, "two joint link" element and "Plastic Wen" link were used for modeling metallic damper.

In OpenSees, "twoNodeLink" element with "Steel02" material was used for modeling of the metallic damper. Braces are modeled using "elasticBeamColumn" command, which are moment-free in both ends. It should be mentioned that the dampers can move only in U2 direction. Details of modeling for this damper are shown in Fig. 15f.

iranpaper Downloaded from https://iranpaper.ir

Table 5
Properties of metallic dampers in each story.

Story	Yield Strength of Damper (kN)	Stiffness of Damper $(\frac{kN}{m})$	Number of Plates
1	375	35,590	14
2	375	35,590	14
3	321	30,506	12
4	321	30,506	12
5	268	25,422	10
6	268	25,422	10
7	134	12,711	5
8	134	12,711	5

The analyses in this study are carried out using two different software (i.e., OpenSees and SAP2000) so that the results from these software can be used to verify the structural modelling and the results obtained from nonlinear analyses. In addition, since the prediction of the total and dissipated energy is not straightforward in OpenSees software, the SAP2000 software can be used to obtain such data that can be used for the performance evaluation of different passive energy dissipation devices.

In order to investigate the accuracy of the results obtained from OpenSees and SAP2000 software, the force–displacement loops of different dampers are predicted under Imperial Valley earthquake. As shown in Fig. 17, the predictions obtained from both software are in good agreement. Also, for each model, period, columns axial force, maximum roof displacement, and maximum roof acceleration were controlled in both software. It was confirmed that for each model, both software almost has the same seismic responses. It should be mentioned that the results presented in this paper were obtained from OpenSees software and only input energy and dissipated energy obtained from SAP2000 software.

4. Numerical results and discussion

4.1. Viscous dampers with different damping coefficient (C)

In this part, linear and nonlinear viscous dampers in diagonal, chevron, and toggle arrangements are compared, which have damping coefficients in accordance to Table 4.

The damping coefficients, C, for different cases are calculated such that an additional damping ratio, ζ , of 15% be available for all arrangements and types of viscous dampers. After analyzing the models using 11 ground motions, the results are represented in Table 6, which are the mean seismic responses under these ground motions. The results indicate that in structures with viscous dampers, the maximum roof displacement and maximum base shear of the structures are reduced approximately by 45% and 40% compared to the primary structure, respectively. Also, in all structures with viscous dampers, the seismic responses of the structures are almost equal, while the damping coefficients are different; this shows that for the same seismic performance level, the diagonal arrangement needs the highest damping coefficient, and the toggle arrangement needs the lowest damping coefficient. It should be noted that the cost of the project will rise when a higher damping coefficient is used. So, for the same seismic performance level, without considering the cost of construction of braces and their connection complexity, the diagonal arrangement has the highest cost and the toggle arrangement has the lowest cost.

4.2. Viscous dampers with an identical damping coefficient (C)

In this part, for a better demonstration of the effect of damping coefficient (C) on seismic responses, the value of C is assumed 839 $\frac{kN.Sec}{m}$ for all arrangements of the viscous damper. This value was chosen so that all arangements of viscous damper are seismically efficient and are in their allowable drift limit. In Figs. 18 and 19, the maximum displacements and maximum base shears of structures are shown, which are obtained from the average of maximum seismic responses of 11 ground motions imposed to the structures. The results show that the structures with viscous damper have significantly smaller displacements and base shears compared to the primary structure without damper. Also, in all arrangements, nonlinear dampers have better seismic performance compared to linear dampers. In the investigation of the arrangement effect, results indicate that the toggle is more efficient than chevron, and chevron is more efficient than diagonal arrangement. Because the values of the magnification factor for diagonal and chevron arrangements are

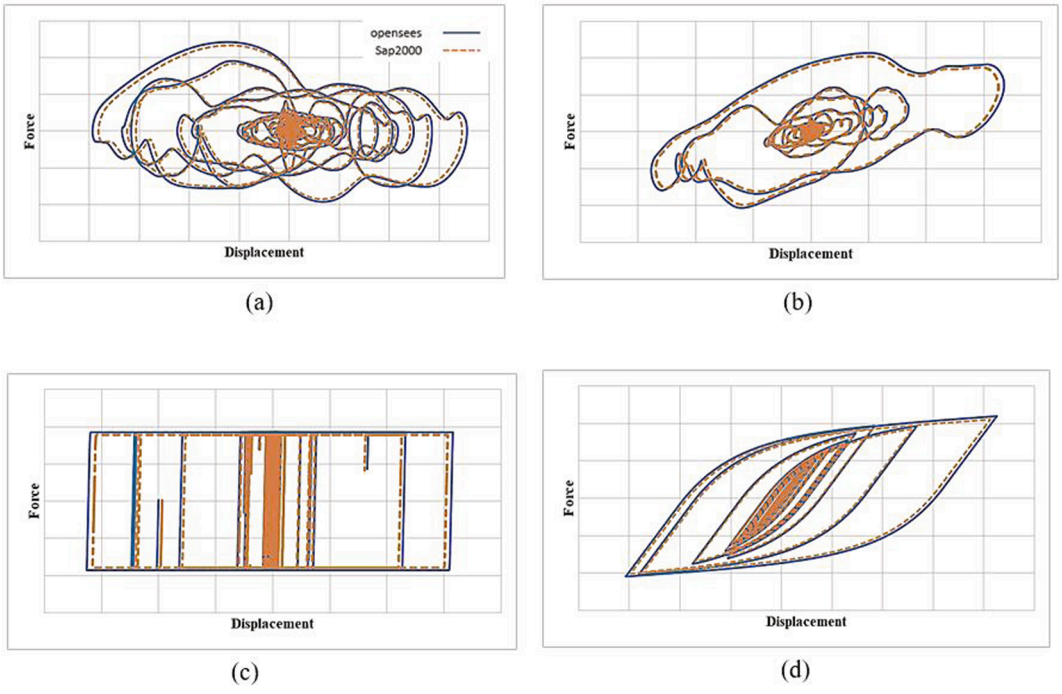

Fig. 17. Force-Displacement loops for: (a) Viscous, (b), Viscoelastic (c), Friction, and (d) Metallic Dampers.

Downloaded from https://iranpaper.ir

Table 6
Seismic responses of viscous dampers in different arrangements.

model	Type	Damping Coefficient $\left(\frac{kN.Sec}{m}\right)$	Maximum Displacement of roof (cm)	Reduction of Displacement (%)	Maximum Base Shear (kN)	Reduction of Base Shear (%)
Primary	–	–	24.50	–	805.0	–
Diagonal	Linear	3157	13.25	45.9	512.5	36.3
	Nonlinear	845	12.50	49.0	517.5	35.7
Chevron	Linear	2458	13.25	45.9	482.5	40.0
	Nonlinear	700	12.85	47.5	467.5	41.9
Toggle	Linear	298	13.60	44.5	480.0	40.3
	Nonlinear	144	12.50	49.0	472.5	41.3

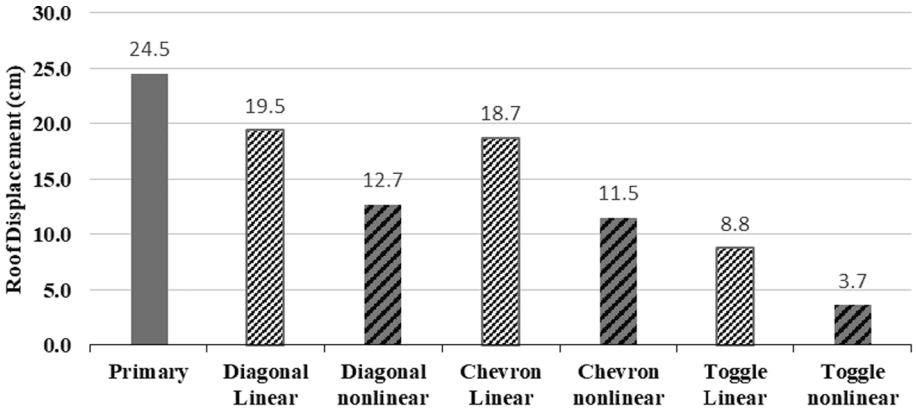

Fig. 18. Maximum displacement of the roof.

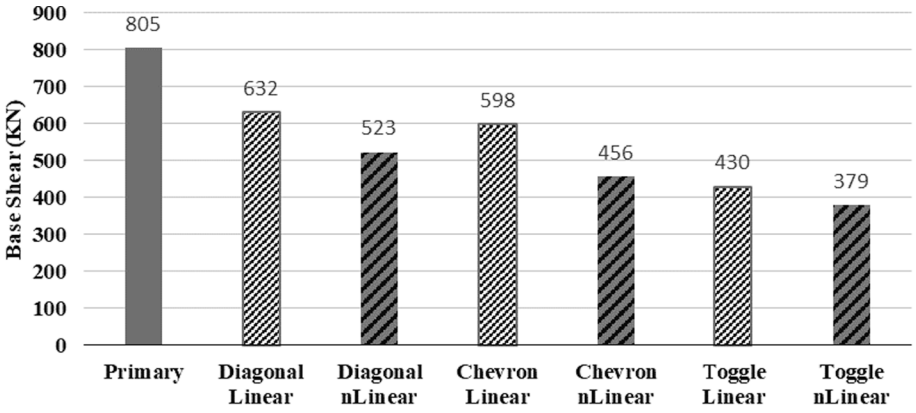

Fig. 19. Maximum base shear.

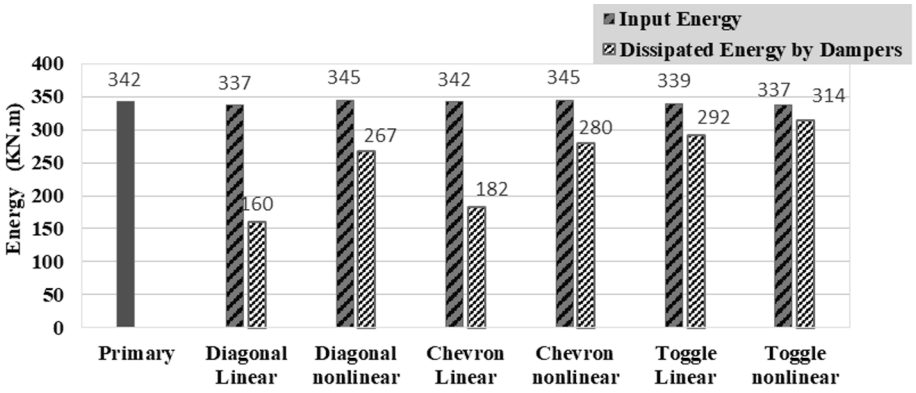

Fig. 20. Input energy and dissipated energy.

Downloaded from https://iranpaper.ir

almost equal, displacement responses for these arrangements have not much difference.

In Fig. 20, the values of input energy into the structure and dissipated energy by dampers are shown, which are obtained from the average of maximum input and dissipated energy of 11 ground motions. Also, for more clarification, in Fig. 21, the ratio of dissipated energy by dampers to input energy is represented. These results show that the nonlinear dampers are more efficient than linear dampers and dissipate much more energy. Besides, from Fig. 20 it is obvious that the toggle arrangement dissipates energy more than the chevron arrangement, and the chevron arrangement dissipates energy more than the diagonal arrangement.

For instance, the displacement and base shear of primary structure and nonlinear toggle arrangement under Imperial Valley ground motion are shown in Figs. 22 and 23, respectively.

In Fig. 24, maximum drift ratio of stories under Imperial Valley ground motion for different arrangements of the viscous damper is shown. The results show that the structures with viscous damper have smaller story drifts compared to the the primary structure. Also, the toggle arrangement has the best performance among the three arrangements of the viscous dampers in reducing the story drifts. Besides, nonlinear dampers are more efficient than linear dampers. In addition, the envelope curves of the maximum displacement of different floors are shown in Fig. 25, which are obtained from the average seismic response of 11 ground motions.

Fig. 26 shows Force-Displacement loops for linear and nonlinear viscous dampers in the first story under Imperial Valley ground motion. There are some noticeable results that can be conferred from this Figure: A) Nonlinear dampers have a larger area of loops in comparison to linear dampers; this means they can dissipate more energy compared to linear dampers. B) Nonlinear dampers have a more stable behavior compared to linear dampers, because their loops are in a smaller range of displacement and a wider range of force. C) Toggle arrangement has the biggest area of loops indicating its superior performance. D) Chevron and Diagonal dampers have loops with the approximately same area that means they have almost similar seismic performance. It should be mentioned that the same performance can be related to their close magnification factors.

4.3. Comparison of seismic demand for metallic, friction, and viscoelastic dampers

While the main goal of this research is to study the influence of the types and arrangements of viscous dampers on the seismic performance of the steel frames, it is also interesting to compare the seismic performance of the structures equipped with different types of dampers including viscoelastic, metallic and friction dampers for the structures under study. There are limited research available to compare the seismic performance of structures equipped with different passive devices and in most studies only the seismic performance of the structures equipped with a specific device is studied. These dampers are designed based on the methods used in practice and therefore, this comparison can provide guidance for engineers in selecting the most efficient energy dissipation devices. However, it should be mentioned that the result of this comparison may be limited to the structural properties used for the case study in this research and general conclusions may not be made without further research.

In this part, the seismic response of metallic, friction, and viscoelastic dampers are compared in Table 7. All properties of these dampers, such as their stiffness and damping coefficient, were discussed in Section 3 of this paper.

As shown in Table 7, all models equipped with dampers have improved seismic performance compared to the primary structure. Among these dampers, the friction damper dissipated the highest amount of energy among others, and the percentage of reduction in displacement demands and base shear are higher for this damper compared to the other dampers of this group. Also, the results indicate that the frames with metallic dampers have smaller displacements and larger base shear compared to the frames equipped with viscoelastic dampers.

In Figs. 27 and 28, maximum story drift ratios under Imperial Valley ground motion and maximum displacement of each story, which are obtained from the average seismic response of 11 ground motions, are shown. The results demonstrate that in all models equipped with dampers, story drift and displacement of each story are reduced in comparison to the primary structure. It is evident from these Figures that the friction damper has the best performance among the dampers of this group. Among the metallic and viscoelastic dampers, metallic dampers show more displacement reduction ability than viscoelastic dampers.

5. Conclusion

In this paper, a total of ten 2D eight-story steel intermediate moment frames equipped with different kinds of dampers were studied (i.e., one frame with no damper, six with linear and nonlinear viscous dampers in three different arrangements, one with viscoelastic, one with friction, and one with a metallic damper). To investigate the seismic behavior of each system, nonlinear time history analyses were performed using eleven ground motion records in OpenSees software. The results based on the cases studied in this paper are presented and compared in three different part:

1) In structures with viscous dampers that are designed and have different damping coefficients, C (i.e., resulting in similar damping ratios, ζ), it was demonstrated that the maximum roof displacement and maximum base shear of the structures are significantly reduced

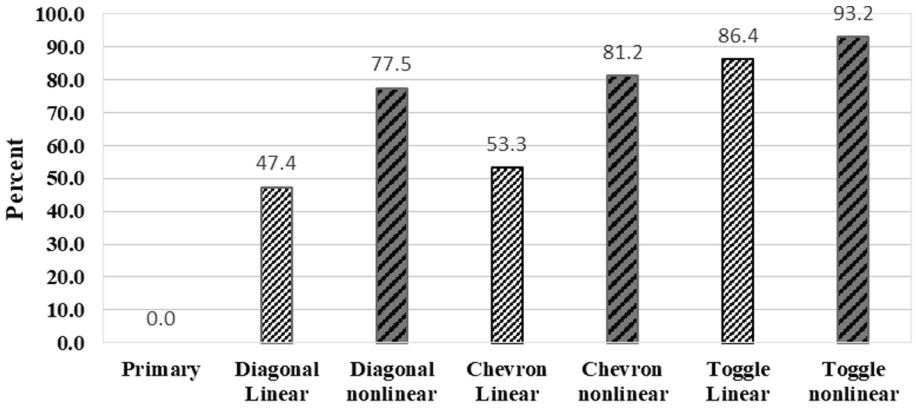

Fig. 21. The ratio of dissipated energy by dampers to input energy.

Downloaded from https://iranpaper.ir

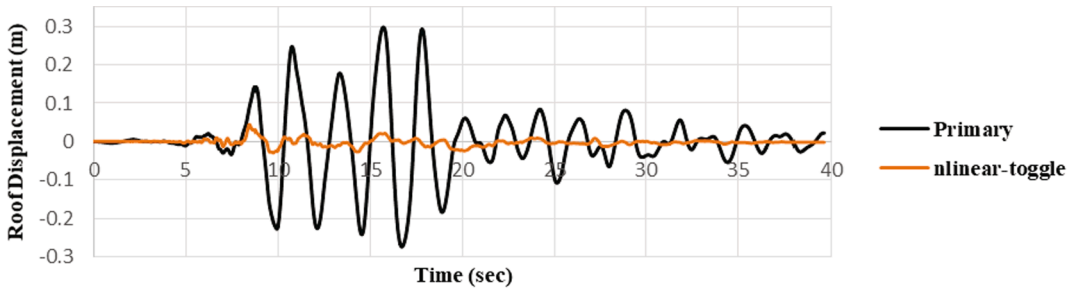

Fig. 22. Displacement of the roof under Imperial Valley ground motion.

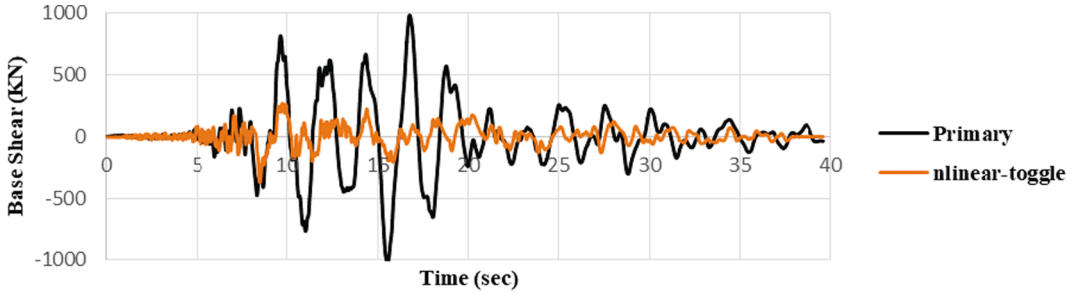

Fig. 23. Base shear under Imperial Valley ground motion.

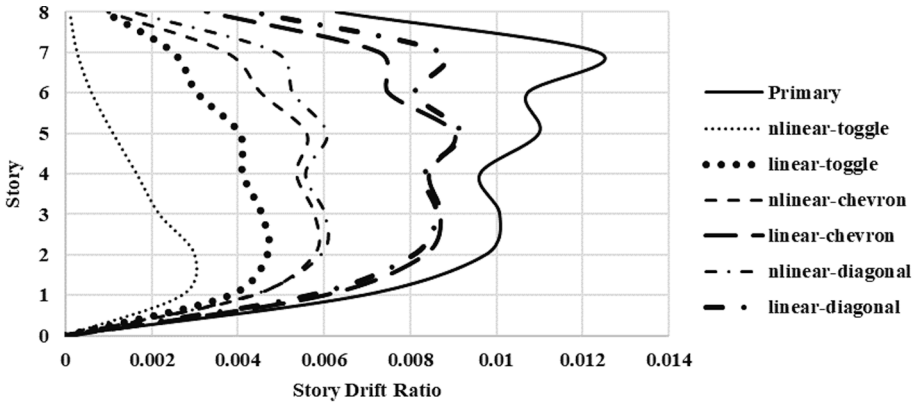

Fig. 24. Maximum story drift ratio under Imperial Valley ground motion.

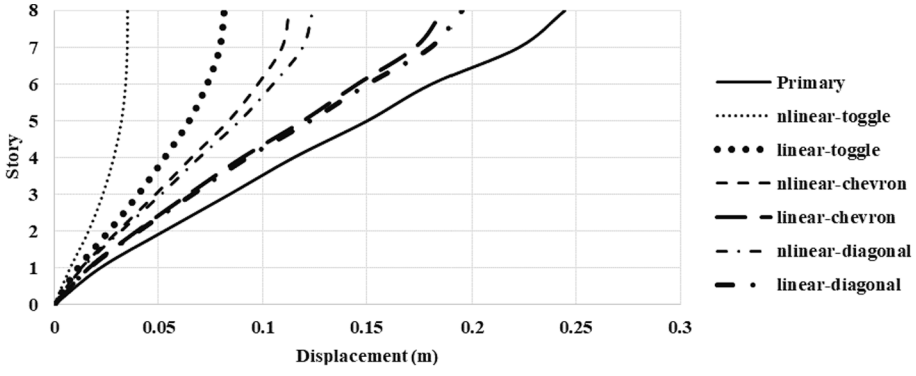

Fig. 25. Maximum displacement in each story.

compared to the primary structure. Also, in these models, the seismic responses of the structures are almost equal, while the damping coefficients are different; this shows that in design for the same seismic performance level, the diagonal arrangement needs the highest damping coefficient, and the toggle arrangement needs the lowest damping coefficient. This suggests that the use of toggle arrangements is more economical, since providing a higher damping coefficient is costly.

Downloaded from https://iranpaper.ir

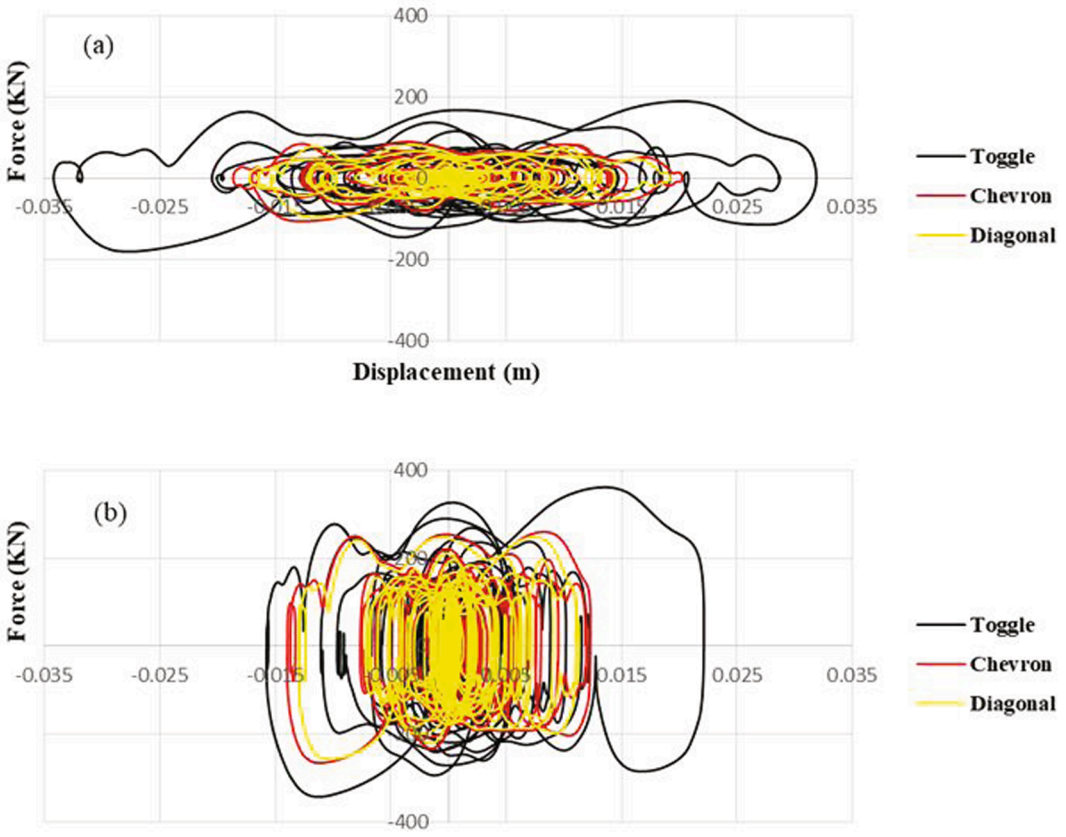

Fig. 26. Force-Displacement loops for different arrangements of viscous damper in the first story under Imperial Valley ground motion: (a) Linear dampers and (b) Nonlinear dampers.

Table 7
Seismic responses of metallic, friction, and viscoelastic dampers.

model	Maximum Displacement of roof (cm)	Reduction of Displacement (%)	Maximum Base Shear (kN)	Reduction of Base Shear (%)
Primary	24.5	–	805	–
Metallic	15.0	38.7	760	5.6
Friction	10.5	57.2	420	47.8
Viscoelastic	18.0	26.5	620	23.3

2) In structures equipped with viscous dampers having the same damping coefficient, C, in all arrangements, nonlinear dampers have a significantly better seismic performance compared to linear dampers. In addition, the effects of different viscous damper arrangements were studied. The results indicated that the toggle arrangement is more efficient than chevron, and chevron is more efficient than diagonal arrangement in terms of displacements, story drifts, base shears and dissipated energy. Also, by evaluating the force–displacement loops of viscous dampers, these results can be conferred: A) Nonlinear dampers have a bigger area of loops in comparison to linear dampers; this means they can dissipate more energy than linear dampers. B) Nonlinear dampers have a more stable behavior than linear dampers because their loops are in a smaller range of displacement and a bigger range of force. C) The toggle arrangement has the largest area under the force–displacement loops and therefore, the farmes equipped with this arrangement can achieve a higher seismic performance in comparison with the other arrangements.

Fig. 27. Maximum story drift ratio under Imperial Valley ground motion.

Downloaded from https://iranpaper.ir

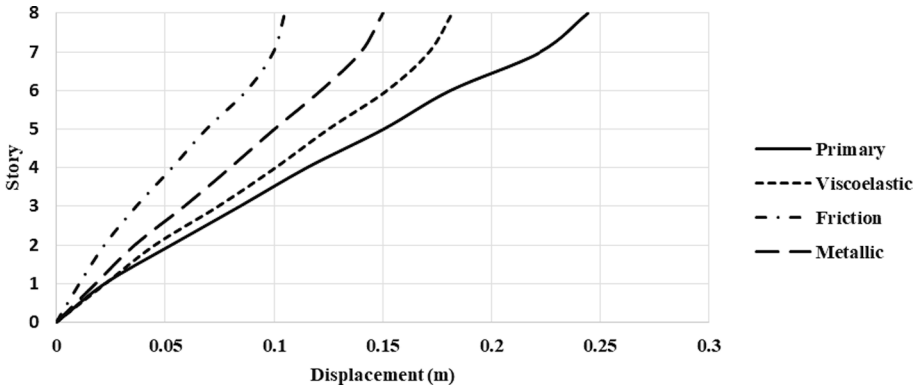

Fig. 28. Maximum displacement in each story.

3) Among the friction, metallic, and viscoelastic dampers, the friction damper dissipated a higher amount of energy compared o the other types of dampers and it had a larger influence on reducing the displacements, story drifts, and base shear compared to the other types of dampers; this can be related to the rectangular hysteresis loops of the friction dampers, which have the largest area of hysteresis loops compared to the other cases.

In summary, among the six different types of viscous dampers studied, the nonlinear viscous damper in toggle arrangement had the best seismic performance. Between all 10 configurations studied in this paper (i.e., viscous, viscoelastic, metallic, and friction dampers), the results showed that the use of the friction damper resulted in the best seismic performance in terms of reducing the seismic demands. Nevertheless, it was evident that regardless of the type of dampers used the seismic performance of the structures improved compared with the original structure, when dampers were used. It is noted that the conclusions made in this paper may be limited to the cases studied and general conclusions may not be made without further research.

Declaration of Competing Interest

The authors declare that they have no known competing financial interests or personal relationships that could have appeared to influence the work reported in this paper.

References

[1] Soong T, Constantinou MC. Passive and Active Vibration Control in Civil Engineering. Department of Civil Engineering State University of New York at Buffalo, editor. CISM Int Centre Mechan Sci 1994.
[2] Scawthorn C, Chen WF. Earthquake Engineering Handbook. CRC Press; 2002.
[3] FEMA. Recommended Provisions: Instructional and Training Materials(FEMA 451B NEHRP). Washington,D.C.; 2006.
[4] Montuori R, Nastri E, Piluso V. Seismic response of EB-frames with inverted Y-scheme: TPMC versus eurocode provisions. Earthq Struct 2015;8(5):1191–214.
[5] Montuori R, Nastri E, Tagliafierro B. Residual displacements for non-degrading bilinear oscillators under seismic actions. Mech Res Commun 2021;111:103651. https://doi.org/10.1016/j.mechrescom.2020.103651.
[6] Montuori R, Nastri E, Piluso V. Rigid-plastic analysis and moment-shear interaction for hierarchy criteria of inverted y EB-Frames. J Constr Steel Res 2014 Apr;1(95):71–80.
[7] Nastri E, Montuori R, Piluso V. Seismic design of MRF-EBF dual systems with vertical links: EC8 vs plastic design. J Earthq Eng 2015;19(3):480–504.
[8] Costanzo S, D'Aniello M, Landolfo R, De MA. Critical discussion on seismic design criteria for cross concentrically braced frames. Ing Sismica. 2018;35(2):23–36.
[9] Costanzo S, D'Aniello M, Landolfo R. Seismic design rules for ductile Eurocode-compliant two-storey X concentrically braced frames. Steel Compos Struct 2020;36(3):273–91.
[10] Costanzo S, D'Aniello M, Landolfo R. The influence of moment resisting beam-to-column connections on seismic behavior of chevron concentrically braced frames. Soil Dyn Earthq Eng 2018;113:136–47.
[11] Constantinou MC, Whittaker AS, Kalpakidis Y, Fenz DM, Warn GP. Performance of Seismic Isolation Hardware under Service and Seismic Loading. MCEER-07-0012; 2007.
[12] Constantinou MC, Symans MD. Experimental study of seismic response of buildings with supplemental fluid dampers. Struct Des Tall Build 1993;2(2):93–132.
[13] Lee D, Taylor DP. Viscous damper development and future trends. Struct Des Tall Build 2001;10(5):311–20.
[14] Uriz P, Whittaker AS. Retrofit of pre-northridge steel moment-resisting frames using fluid viscous dampers. Struct Des Tall Build 2001;10(5):371–90.
[15] Miyamoto HK, Gilani ASJ, Wada A, Ariyaratana C. Collapse risk of tall steel moment frame buildings with viscous dampers subjected to large earthquakes- Part I: Damper limit states and failure modes of 10-storey archetypes. Struct Des Tall Spec Build 2010 Jun 1;19(4):421–38.
[16] Kim J, Lee S, Choi H. Progressive collapse resisting capacity of moment frames with viscous dampers. Struct Des Tall Spec Build 2013;22(5):399–414.
[17] Wang S, Mahin SA. Seismic retrofit of a high-rise steel moment-resisting frame using fluid viscous dampers. Struct Des Tall Spec Build 2017;26(10):e1367. https://doi.org/10.1002/tal.v26.1010.1002/tal.1367.
[18] Sepehri A, Taghikhany T, Ahmadi Namin SMR. Seismic design and assessment of structures with viscous dampers at limit state levels: Focus on probability of damage in devices. Struct Des Tall Spec Build 2019;28(1):e1569. https://doi.org/10.1002/tal.v28.110.1002/tal.1569.
[19] Gong S, Zhou Y, Ge P. Seismic analysis for tall and irregular temple buildings: A case study of strong nonlinear viscoelastic dampers. Struct Des Tall Spec Build 2017;26(7):e1352. https://doi.org/10.1002/tal.v26.710.1002/tal.1352.
[20] Heydarinouri H, Zahrai SM. Iterative step-by-step procedure for optimal placement and design of viscoelastic dampers to improve damping ratio. Struct Des Tall Spec Build 2017;26(9):e1361. https://doi.org/10.1002/tal.v26.910.1002/tal.1361.
[21] LIAO WEN-I, MUALLA IMAD, LOH CHIN-HSIUNG. Shaking-table test of a friction-damped frame structure. Struct Des Tall Spec Build 2004;13(1):45–54.
[22] Ribakov Y. Using viscous and variable friction dampers for improving structural seismic response. Struct Des Tall Spec Build 2011 Aug 1;20(5):579–93.
[23] Tafakori E, Banazadeh M, Jalali SA, Tehranizadeh M. Risk-based optimal retrofit of a tall steel building by using friction dampers. Struct Des Tall Spec Build 2013;22(9):700–17.
[24] Brando G, D'Agostino F, De Matteis G. Seismic performance of MR frames protected by viscous or hysteretic dampers. Struct Des Tall Spec Build 2015;24(9):653–71.
[25] Bagheri S, Barghian M, Saieri F, Farzinfar A. U-shaped metallic-yielding damper in building structures: Seismic behavior and comparison with a friction damper. Structures. 2015 Aug;1(3):163–71.
[26] Tehrani P, Maalek S. Comparison of nonlinear static and nonlinear dynamic analyses in the estimation of the maximum displacement for structures equipped with various damping devices. 4th Int Conf Earthq Eng Taipei. Taiwan 2006:129.
[27] Tehrani P, Maalek S. The use of passive dampers and conventional strengthening methods for the rehabilitation of an existing steel structure. 4th International Conference on Earthquake Engineering. Taipei, Taiwan; 2006.
[28] Nastri E, D'Aniello M, Zimbru M, Streppone S, Landolfo R, Montuori R, et al. Seismic response of steel Moment Resisting Frames equipped with friction beam-to-column joints. Soil Dyn Earthq Eng 2019;119:144–57.
[29] Mirzai NM, Attarnejad R, Hu JW. Enhancing the seismic performance of EBFs with vertical shear link using a new self-centering damper. Ing Sismica 2018;35(4):57–76.
[30] Titirla M, Katakalos K, Zuccaro G, Fabbroccino F. On the mechanical modeling of an innovative energy dissipation device. Ing Sismica 2017;34(2):126–37.
[31] Piluso V, Montuori R, Nastri E, Paciello A. Seismic response of MRF-CBF dual systems equipped with low damage friction connections. J Constr Steel Res 2019;154:263–77.
[32] Constantinou MC, Tsopelas P, Hammel W, Sigaher AN. Toggle-brace-damper seismic energy dissipation systems. J Struct Eng 2001;127(2):105–12.
[33] Zhang R, He H, Weng D, Zhou H, Ding S. Theoretical analysis and experimental research on toggle-brace-damper system considering different installation modes. Sci Iran 2012;19(6):1379–90.
[34] Hwang J-S, Huang Y-N, Hung Y-H. Analytical and Experimental Study of Toggle-Brace-Damper Systems. J Struct Eng 2005;131(7):1035–43.
[35] Constantinou M, Soong T, Dargush G. Passive energy dissipation systems for structural design and retrofit; 1998.

Downloaded from https://iranpaper.ir

[36] Soong T, Dargush G. Passive energy dissipation systems in structural engineering; 1997.
[37] Hwang J-S, Huang Y-N, Yi S-L, Ho S-Y. Design Formulations for Supplemental Viscous Dampers to Building Structures. J Struct Eng 2008;134(1):22–31.
[38] Chang K, Lin Y, Lai M. Seismic analysis and design of structures with viscoelastic dampers. ISET J Earthq Technol 1998;35(4):143–66.
[39] Pall AS, Marsh C. Response of friction damped braced frames. J Struct Eng 1982; 108(9):1313–23.
[40] Pall A. Performance-based design using pall friction dampers-an economical design solution. 13th World Conf Earthq Eng 2004;70(7):571–6.
[41] Alehashem SSM, Keyhani A, Pourmohammad H. Behavior and performance of structures equipped with ADAS & TADAS dampers (a comparison with conventional structures). 14th World Conf Earthq Eng 2008:12–7.
[42] Ramirez OM, Constantinou MC, Kircher CA, Whittaker A, Johnson MW, Gomez J, et al. Development and evaluation of simplified procedures for the analysis and design of buildings with passive energy dissipation systems; 2001.
[43] American Society of Civil Engineers (ASCE). Minimum Design Loads and Associated Criteria for Buildings and Other Structures, ASCE/SEI 7-16; 2016.
[44] American Institute of Steel Construction. Specification for Structural Steel Buildings (ANSI/AISC 360-16); 2016.
[45] American Institute of Steel Construction. Seismic Provisions for Structural Steel Buildings (ANSI/AISC 341-16); 2016.
[46] Federal Emergency Management Agency(FEMA). Quantification of building seismic performance factors(FEMA P695); 2009.
[47] SAP2000. Comput Struct Inc.
[48] Pacific Earthquake Engineering Research (PEER) Center. Open System for Earthquake Engineering Simulation(OpenSees).
[49] American Society of Civil Engineers. Seismic Evaluation and Retrofit of Existing Buildings(ASCE/SEI 41-17). 2017 Dec.
[50] Filiatrault A, Cherry S. Seismic Design Spectra for Friction-Damped Structures. J Struct Eng 1990;116(5):1334–55.
[51] Tsai K-C, Chen H-W, Hong C-P, Su Y-F. Design of Steel Triangular Plate Energy Absorbers for Seismic-Resistant Construction. Earthq Spectra 1993;9(3):505–28.